The Astronomical Journal, 141:21 (11pp), 2011 January doi:10.1088/0004-6256/141/1/21

THE SOLAR NEIGHBORHOOD. XXIII. CCD PHOTOMETRIC DISTANCE ESTIMATES OF SCR TARGETS—77 M DWARF SYSTEMS WITHIN 25 pc

Jennifer G. Winters[1,5], Todd J. Henry[1,5], Wei-Chun Jao[1,5], John P. Subasavage[2,5], Charlie T. Finch[3,5], and Nigel C. Hambly[4]

[1] Department of Physics and Astronomy, Georgia State University, Atlanta, GA 30302-4106, USA; winters@chara.gsu.edu, thenry@chara.gsu.edu, jao@chara.gsu.edu
[2] Cerro Tololo Inter-American Observatory, Casilla 603, La Serena, Chile; jsubasavage@ctio.noao.edu
[3] United States Naval Observatory, Washington, DC 20392-5420, USA; finch@usno.navy.mil
[4] Scottish Universities Physics Alliance (SUPA), Institute of Astronomy, University of Edinburgh, Royal Observatory, Blackford Hill, Edinburgh EH9 3HJ, UK; nch@roe.ac.uk
Received 2010 August 23; accepted 2010 October 18; published 2010 December 10

ABSTRACT

We present CCD photometric distance estimates of 100 SCR (SuperCOSMOS RECONS) systems with $\mu \geqslant 0\farcs18$ yr^{-1}, 29 of which are new discoveries previously unpublished in this series of papers. These distances are estimated using a combination of new *VRI* photometry acquired at CTIO and *JHK* magnitudes extracted from 2MASS. The estimates are improvements over those determined using photographic plate *BRI* magnitudes from SuperCOSMOS plus *JHK*, as presented in the original discovery papers. In total, 77 of the 100 systems investigated are predicted to be within 25 pc. If all 77 systems are confirmed to have $\pi_{\rm trig} \geqslant 40$ mas, this sample would represent a 23% increase in M dwarf systems nearer than 25 pc in the southern sky.

Key words: solar neighborhood – stars: distances – stars: low-mass – stars: statistics – techniques: photometric

1. INTRODUCTION

For more than a century, there has been serious effort invested in compiling a complete survey of stars near the Sun. Recent work of note includes Lépine's SUPERBLINK program that has detected dwarfs, giants, and subgiants in the northern sky with spectroscopic distances $\leqslant$ 25.0 pc (Lépine 2005b) and additional objects in the south, but without spectral types or distance estimates (Lépine 2005a, 2008). Reid and collaborators have also made progress in this area, focusing on objects within 20 pc using spectrophotometry, as reported in the Meeting the Cool Neighbors papers (Reid et al. 2008, and references therein). These efforts include both previously known and new members of the solar neighborhood. The survey most similar to our survey discussed here is that of Deacon who used SuperCOSMOS *I* plates and Two Micron All Sky Survey (2MASS) to reveal new nearby red objects in the southern sky (Deacon et al. 2005; Deacon & Hambly 2007). This paper focuses specifically on new discoveries from our SuperCOSMOS RECONS (SCR) effort (Hambly et al. 2004; Henry et al. 2004; Subasavage et al. 2005a, 2005b; Finch et al. 2007).

The most widespread method of revealing new members in the Sun's vicinity is through proper motion searches, as nearby objects generally have larger proper motions than those further away. Much of the nearby star work in the latter half of the 20th century was based upon the Palomar and UK Schmidt sky surveys performed by Luyten (1979a, 1979b) and the Lowell proper motion surveys by Giclas et al. (1971, 1978a, 1978b). Long-term efforts to obtain optical photometry by Weis (1996) in the northern hemisphere and Eggen (1987) in the southern hemisphere were carried out by observing one star at a time. This photometry is often used to estimate distances to stars using various color–absolute magnitude calibrations. Much of these data were then incorporated into the Catalog of Nearby Stars (CNS; Gliese & Jahreiß 1991), which provided a snapshot view of the solar neighborhood population, albeit one that was incomplete. NStars continued in this vein with a comprehensive database of objects with trigonometric parallaxes (see Henry et al. 2002, 2003 for more complete discussions). As we entered the 21st century, large sky surveys such as 2MASS (Skrutskie et al. 2006), DENIS (The Denis Consortium 2005), and SDSS (Adelman-McCarthy et al. 2009) gathered magnitudes in optical and infrared filters of huge numbers of sources that could be examined for nearby star candidates.

Once a new nearby star candidate is found, distances can be determined using a variety of astrometric, photometric, and spectrophotometric techniques. In this paper, we focus on distance estimates made using photometry from a combination of optical CCDs and infrared arrays, which is an effective intermediate method for refining membership of the solar neighborhood. This method provides distances that are more accurate than those determined using photographic plates, but that are not as precise (or as time and labor intensive) as those calculated via trigonometric parallax.

A primary goal of the RECONS group (the Research Consortium on Nearby Stars[6]) is to identify hidden members of the solar neighborhood within 25 pc to match the horizons of the CNS and NStars efforts. We have focused our searches in the southern hemisphere because that portion of the sky has been historically underrepresented and is expected to yield rich treasures in the form of new stellar neighbors. In this paper, we first discuss recent photometric distance efforts by others (Section 2), then provide descriptions of our two methods used to estimate distances photometrically: via scanned photographic plates (Section 3) and improvements based on CCD photometry (Section 4), with complementary spectroscopy (Section 5). We sum up the results in Section 6.

[5] Visiting Astronomer, Cerro Tololo Inter-American Observatory. CTIO is operated by AURA, Inc. under contract to the National Science Foundation.

[6] http://www.recons.org.

Table 1
Recent Photometric Distance Estimation Efforts in the Southern Sky

Source	No. of Systems	Reference
NStars	329[a]	1,2
Phan-Bao et al.	37	3,4,5,6,7
Reylé et al.	34	8,9
Finch et al.	15	10
Costa & Méndez	3	11
RECONS (plate phot)	**100**	12,13,14,15,16,*
RECONS (CCD phot)	**77**	*

Notes.
[a] Trigonometric parallaxes $\geqslant$40 mas.
References. (1) NStars Database, see Henry et al. 2002; (2) NStars Database, see Henry et al. 2003; (3) Delfosse et al. 2001; (4) Phan-Bao et al. 2001; (5) Phan-Bao et al. 2003; (6) Phan-Bao et al. 2006; (7) Phan-Bao et al. 2008; (8) Reylé et al. 2002; (9) Reylé & Robin 2004; (10) Finch et al. 2010; (11) Costa & Méndez 2003; (12) Hambly et al. 2004; (13) Henry et al. 2004; (14) Subasavage et al. 2005a; (15) Subasavage et al. 2005b; (16) Finch et al. 2007; (*): this paper.

2. RECENT PHOTOMETRIC DISTANCE EFFORTS BY OTHERS

Table 1 lists the main photometric distance estimation efforts in the southern sky since the NStars Database was compiled. The efforts considered are purely photometric and are independent of any spectral types or relations based on spectroscopy. The criteria for inclusion in the counts are that the systems (1) be new discoveries, (2) have colors of red dwarfs (effectively spectral type M, $(V-K) \gtrsim 3.0$), (3) be found in the southern hemisphere (decl. $\leqslant 0^\circ$), and (4) are estimated to be within 25.0 pc via a photometric distance estimate.

We used the NStars Database as a benchmark to evaluate solar neighborhood completeness, as NStars incorporated only those objects for which a parallax had been measured; therefore, it was the most definitive collection of systems found within 25 pc. Great care was taken when extracting the sample of 329 southern M dwarf systems from NStars. All northern hemisphere objects, as well as those objects brighter than $M_V = 9.00$, the adopted cutoff for the brightest M dwarfs, were eliminated. For the remaining objects with no designated spectral type, various colors such as $(V-I)$, $(V-J)$, and $(J-K)$, depending on the availability of photometry, were used to eliminate white dwarfs that remained in the sample. If the primary component of a multiple system was discovered to be anything other than an M dwarf, or if the system contained a white dwarf, the system was omitted. Finally, the individual components of multiple systems were combined to give a count of southern M dwarf systems.

Figure 1 shows results from these photometric distance efforts in concert with the 329 systems from NStars (small dots). Declination is plotted against right ascension in a polar plot with R.A. progressing counterclockwise from 0 to 24 hr and decl. starting at 0° at the outer boundary and moving inward to −90° at the center. Phan-Bao's 37 objects[7] are denoted by open triangles, Reylé's 34 objects[8] are denoted by open circles,

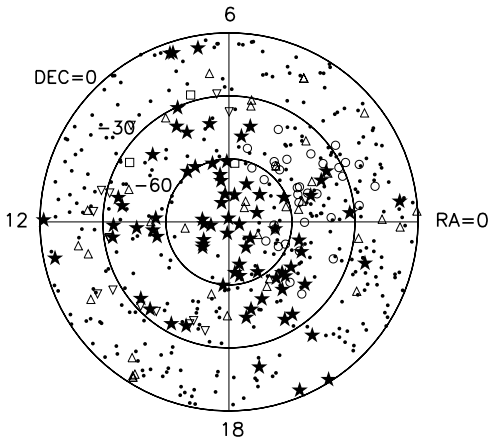

Figure 1. Polar plot for southern hemisphere photometric distance estimates of objects within 25.0 pc, where R.A. advances counterclockwise from 0 to 24 hr, and decl. ranges from 0° at the outer edge to −90° in the center. The 329 red dwarf primaries with trigonometric parallaxes from NStars are noted as small solid black dots; Phan-Bao et al. results are shown as 37 open triangles; Reylé et al. results are shown as 34 open circles; Finch et al. results are 15 open upside-down triangles; Costa & Méndez results are three open squares; RECONS's SCR results are shown as 77 solid stars from this paper with CCD photometric distance estimates.

Finch's 15 objects[9] are noted by upside-down open triangles, and Costa & Méndez's three objects[10] are indicated with open squares. The 77 systems found to date in SCR surveys (discussed in the next section) are represented by solid stars. In all cases, the counts and points in Figure 1 represent newly discovered southern systems.

3. DEFINITION OF THE SCR SAMPLE

SCR objects are previously undiscovered systems that have been revealed through searches utilizing the digitally scanned SuperCOSMOS photographic plates. A sample of 72 star systems was harvested from five earlier papers in this series (Hambly et al. 2004; Henry et al. 2004; Subasavage et al. 2005a, 2005b; Finch et al. 2007). To date, an additional 28 systems have been found during continuing searches and are reported here for the first time. Table 2 lists the names, coordinates, and SuperCOSMOS B_J, R_{59F}, and I_{IVN} plate magnitudes. Additional data for these objects are found in Table 3.

The 100 SCR systems (104 objects) listed in Table 3 comprise all SCR red dwarfs with proper motions $\geqslant 0\farcs18$ yr^{-1} estimated to be within 25.0 pc based upon "plate distance estimates." These estimates use SuperCOSMOS B_J, R_{59F}, and I_{IVN} plate magnitudes (hereafter *BRI*) and JHK_s[11] magnitudes from 2MASS. The 100 systems all have M dwarf primaries, two of which are binaries with separations large enough to permit separate plate distance estimates for the secondaries, SCR2241-6119B and SCR2335-6433B. Two additional objects, SCR1107-3420B and SCR1746-8211, have CCD distance estimates that place them within 25.0 pc, but they are not included in the counts of M dwarf discoveries because the primary of the system is not an M dwarf.

In Table 3, Columns 1–3 are the names, R.A., and decl. (epoch and equinox 2000.0). Columns 4 and 5 are the proper motions

[7] In the case of Phan-Bao et al. (2001), where two different distances were given, we used the Dist_I that they considered more dependable. Their photometric distances were estimated using DENIS $I-J$ colors with errors ∼15%–45%.
[8] In the case of Reylé et al., we used only those distance estimates that were unambiguously within 25.0 pc, i.e., we do not count those stars with multiple estimates in Reylé et al. (2002). Their photometric distances were estimated using DENIS $I-J$ colors with errors up to 45%.
[9] Finch's photometric distances are based on SuperCOSMOS *BRI* and 2MASS *JHK* photometry and were estimated using a method identical to that discussed in this paper for plate photometry estimates.
[10] The photometric distances were estimated using M_V versus $V-R$ and M_V versus $V-I$ relations derived in Henry et al. (2004), with errors ∼15%.
[11] Henceforth, the subscript on the 2MASS K_s filter will be dropped.

Table 2
BRI Photometric Results for New SCR Discoveries

Name	R.A.	Decl.	B_J	R_{59F}	I_{IVN}
SCR0017-3219	00 17 15.73	−32 19 54.0	16.80	14.59	12.48
SCR0027-0806	00 27 45.36	−08 06 04.7	18.65	16.26	13.49
SCR0113-7603	01 13 31.47	−76 03 09.3	17.68	15.23	13.05
SCR0137-4148	01 37 23.49	−41 48 56.2	16.91	14.55	12.24
SCR0150-3741	01 50 13.25	−37 41 52.0	15.80	13.49	11.41
SCR0214-0733	02 14 44.69	−07 33 24.7	...	9.71	8.82
SCR0325-0308	03 25 03.09	−03 08 20.4	15.22	13.17	11.39
SCR0506-4712	05 06 07.29	−47 12 51.6	14.07	11.96	10.32
SCR0509-4325	05 09 43.85	−43 25 17.4	15.12	13.00	10.71
SCR0513-7653	05 13 05.97	−76 53 21.9	14.54	12.32	11.23
SCR0526-4851	05 26 40.80	−48 51 47.3	13.82	11.67	10.02
SCR0607-6115	06 07 58.09	−61 15 10.5	15.75	13.43	11.13
SCR0643-7003	06 43 29.79	−70 03 20.8	13.95	11.51	9.75
SCR0644-4223AB	06 44 32.09	−42 23 45.2	15.59J	13.35J	11.18J
SCR0713-0511	07 13 11.23	−05 11 48.6	11.76	9.31	8.84
SCR1107-3420B	11 07 50.25	−34 21 00.6	16.35	14.15	11.81
SCR1932-0652	19 32 46.33	−06 52 18.1	14.92	13.27	11.50
SCR2009-0113	20 09 18.24	−01 13 38.2	15.36	13.09	10.62
SCR2018-3635	20 18 06.52	−36 35 27.7	16.31	14.07	11.47
SCR2025-2259	20 25 18.93	−22 59 06.0	15.26	13.26	11.40
SCR2033-4903	20 33 01.87	−49 03 10.6	16.57	14.17	11.34
SCR2104-5248	21 04 53.85	−52 48 34.3	14.72	12.75	10.94
SCR2105-5503	21 05 13.78	−55 03 56.3	15.01	12.96	10.76
SCR2122-4314	21 22 16.92	−43 14 05.0	14.26	12.06	10.01
SCR2135-5325	21 35 39.63	−53 25 31.5	17.43	15.07	12.30
SCR2142-7405	21 42 58.54	−74 05 55.5	14.24	12.20	10.59
SCR2252-2220	22 52 25.82	−22 20 06.8	14.95	12.82	10.85
SCR2301-5530	23 01 32.51	−55 30 17.6	14.06	12.24	10.25
SCR2325-6740	23 25 25.13	−67 40 07.9	15.60	13.32	11.09

Notes. Coordinates are epoch and equinox 2000.0 using SuperCOSMOS positions transformed to epoch 2000.0 using the proper motions and position angles listed here; if AB, photometry or spectral type is for the system, i.e., joint. In the case of SCR0214-0733, no *B* plate magnitude was available in SuperCOSMOS.

and position angles as measured by SuperCOSMOS. Columns 6–9 list the *VRI* magnitudes and the number of nights each system was observed. The 2MASS *JHK* magnitudes are listed in Columns 10–12. Columns 13–18 provide the plate distance estimates, related errors, and number of color–absolute magnitude relations utilized (see next paragraph), followed by the CCD distance estimates (see Section 4.3), the corresponding errors, and number of relations utilized. The tangential velocities, based on the CCD distance estimates and the SuperCOSMOS proper motions, are given in Column 19. Column 20 lists the spectral types, where available, and Column 21 includes the references for the publications that originally reported each object, where the 29 new objects in this paper are noted with reference 6. A final Column 22 is provided for notes.

A system's plate distance estimate determines its membership in this sample and is based on up to 11 useful M_K versus color relations, as described in Hambly et al. (2004). Relevant errors in the SuperCOSMOS plate photometry for this sample, based on the ranges in *BRI* magnitudes for the sources, are 0.2–0.6 mag for $B = 11$–21, 0.1–0.3 mag for $R = 9$–18, and 0.2–0.4 mag for $I = 8$–16 (Hambly et al. 2001). The errors on the individual passbands are largely systematic in origin and are correlated between the passbands because of the calibration technique used; however, the errors on colors such as $(B - R)$ and $(R - I)$ are smaller, which is more important for their use in distance–color relations (see also Section 4.4).

A plate distance estimate is considered reliable if all 11 relations are applicable, i.e., if a star's color falls within the range covered by the calibrations detailed in Hambly et al. (2004) for single, main-sequence stars. Between six and ten relations indicates that the distance estimate is indicative, but less reliable. Six relations are adopted because if one plate magnitude is erroneous, up to five relations may drop out. Thus, if at least six relations are valid, then at least two of the three *BRI* magnitudes provide optical/infrared colors consistent with normal main-sequence stars. In the present sample, only two stars have fewer than six valid relations, so their distance estimates are highly suspect. In fact, the improved distance estimates discussed next indicate that both are beyond 50 pc.

4. IMPROVING THE DISTANCE ESTIMATES

4.1. VRI CCD Photometry

Our goal was to obtain at least two sets of V_J, R_{KC} and I_{KC}[12] (hereafter *VRI*) photometry for all 104 objects to improve our distance estimates. These new distance estimates are dubbed "CCD distance estimates" to reflect the combination of CCD photometry at *VRI* and 2MASS photometry at *JHK*, and all *R* and *I* magnitudes refer to CCD values for the remainder of this paper.

Care is taken during a night of photometry to ensure that previously observed objects are sandwiched between targets that are new to the program. Multiple results for a single object are then compared to ensure consistency and can also be used to indicate possible variability. The photometric observations used in making the distance estimates reported here span a seven year interval from 2003 January through 2010 May.[13] In total, over 800 frames were acquired on the 0.9 m telescope at the Cerro Tololo Inter-American Observatory (CTIO) for this study. A small subset of 16 frames was acquired on the CTIO 1.0 m in 2005 August; results are consistent to 0.03 mag with the 0.9 m data.

All data were reduced using IRAF. Calibration frames taken at the beginning of each night were used for typical bias subtraction and dome flat fielding. Standard star fields from Graham (1982), Bessel (1990), and/or Landolt (1992, 2007) were observed multiple times each night in order to derive transformation equations and extinction curves. In order to match those used by Landolt, apertures 14″ in diameter were used to determine the stellar fluxes, except in cases where close contaminating sources needed to be deconvolved. In these cases, smaller apertures were used, and aperture corrections were applied. Further details about the data reduction procedures, transformation equations, etc., can be found in Jao et al. (2005).

Figures 2–4 illustrate the total errors versus magnitude in each of the three filters for the 268 stars with three or more nights of photometry from our program, including some of the SCR stars reported here. These errors incorporate signal-to-noise errors, nightly errors determined by fits to standard stars, and night-to-night measurement differences to provide a comprehensive assessment of our photometric errors. Signal-to-noise errors are

[12] Subscript: J, Johnson; KC, Kron–Cousins. The central wavelengths for V_J, R_{KC}, and I_{KC} are 5475 Å, 6425 Å, and 8075 Å, respectively.

[13] On the CTIO 0.9 m, the Tek 2 *VRI* filter set was used; however, the Tek 2 *V* filter originally used cracked in 2005 March and was replaced by the very similar Tek 1 *V* filter. Reductions indicate no significant differences in the photometric results from the two filters, as discussed in detail in Jao et al. (2010). On the CTIO 1.0 m, the Y4KCam filter set was used that contains the same filters as those on the 0.9 m.

Table 3
Photometric Results for SCR Sample

Name	R.A.	Decl.	μ	P.A.	V_J	R_{KC}	I_{KC}	No. of Nights	J	H	K_s	d_{plt}	σ_{plt}	No. of Relations	d_{ccd}	σ_{ccd}	No. of Relations	V_{tan}	SpType	Reference	Notes
			($''$yr^{-1})	(°)								(pc)	(pc)		(pc)	(pc)		(km s^{-1})			
(1)	(2)	(3)	(4)	(5)	(6)	(7)	(8)	(9)	(10)	(11)	(12)	(13)	(14)	(15)	(16)	(17)	(18)	(19)	(20)	(21)	(22)
SCR0017-3219	00 17 15.73	−32 19 54.0	0.220	096.9	15.45	14.11	12.39	2	10.64	10.08	9.73	21.0	7.3	11	21.3	3.4	12	22.2	...	6	
SCR0027-0806	00 27 45.36	−08 06 04.7	0.184	122.3	17.51	15.83	13.72	2	11.57	10.97	10.61	22.9	6.6	11	18.6	2.9	12	16.2	...	6	
SCR0111-4908	01 11 47.52	−49 08 08.9	0.542	213.1	17.72	15.92	13.75	2	11.54	11.00	10.61	23.6	10.8	11	17.6	2.8	12	45.1	M5.5V	3	
SCR0113-7603	01 13 31.47	−76 03 09.3	0.228	125.1	16.07	14.62	12.83	2	11.03	10.47	10.13	21.7	5.6	11	22.8	3.6	12	24.6	...	6	
SCR0135-6127	01 35 53.66	−61 27 11.1	0.255	256.8	14.32	13.11	11.57	2	10.06	9.53	9.24	20.9	7.8	11	24.8	3.8	12	30.0	M3.5V	5	
SCR0137-4148	01 37 23.49	−41 48 56.2	0.238	054.3	15.33	13.99	12.30	2	10.68	10.07	9.78	21.8	6.3	11	24.1	3.8	12	27.2	...	6	
SCR0138-5353	01 38 20.51	−53 53 26.1	0.297	071.0	14.36	13.20	11.70	2	10.28	9.69	9.42	24.3	7.4	11	29.7	4.6	12	41.8	M3.5V	5	
SCR0150-3741	01 50 13.25	−37 41 52.0	0.230	112.3	14.47	13.23	11.64	2	10.11	9.54	9.24	21.5	6.0	11	22.8	3.5	12	24.9	...	6	
SCR0211-6108	02 11 35.42	−61 08 53.8	0.234	060.8	10.40	9.84	9.37	2	8.67	8.15	8.07	23.0	6.1	3	58.5	9.0	6	64.9	K2.0V	5	
SCR0214-0733	02 14 44.69	−07 33 24.7	0.399	128.9	9.89	9.35	8.88	2	8.20	7.80	7.60	21.2	8.3	7	47.3	7.3	6	89.5	K1.0V	6	a
SCR0232-8458	02 32 50.12	−84 58 09.5	0.220	141.9	11.47	10.65	9.90	2	9.00	8.34	8.18	25.0	8.9	6	43.3	7.2	8	45.2	K8.0V	5	
SCR0246-7024	02 46 02.25	−70 24 06.3	0.259	113.2	14.86	13.44	11.61	4	9.84	9.33	9.02	20.0	8.1	11	14.2	2.3	12	17.5	M4.5V	5	
SCR0325-0308	03 25 03.09	−03 08 20.4	0.197	082.7	13.88	12.79	11.41	2	10.06	9.45	9.20	24.8	7.4	11	31.5	4.9	12	29.4	...	6	
SCR0420-7005	04 20 12.55	−70 05 58.7	0.670	021.2	17.09	15.35	13.25	3	11.19	10.59	10.25	22.5	9.2	11	16.3	2.7	12	51.8	M5.5V	2, 3	
SCR0506-4712	05 06 07.29	−47 12 51.6	0.207	319.4	12.63	11.65	10.46	2	9.32	8.66	8.43	21.1	5.7	11	30.2	4.9	12	29.7	...	6	
SCR0509-4325	05 09 43.85	−43 25 17.4	0.225	324.9	14.09	12.83	11.21	2	9.61	9.00	8.74	18.0	5.2	11	16.5	2.6	12	17.6	...	6	
SCR0513-7653	05 13 05.97	−76 53 21.9	0.274	301.2	12.99	11.89	10.52	2	9.24	8.63	8.36	16.2	8.6	11	22.6	3.6	12	29.4	...	6	
SCR0526-4851	05 26 40.80	−48 51 47.3	0.279	158.7	12.88	11.79	10.43	2	9.10	8.46	8.24	20.1	5.3	11	20.7	3.3	12	27.3	...	6	
SCR0527-7231	05 27 06.99	−72 31 20.0	0.368	018.3	14.71	13.49	11.86	3	10.34	9.76	9.47	22.7	6.5	11	25.1	3.9	12	43.8	M3.5V	5	
SCR0607-6115	06 07 58.09	−61 15 10.5	0.217	008.5	14.57	13.26	11.57	2	9.98	9.38	9.10	19.8	5.9	11	18.4	2.9	12	18.9	...	6	
SCR0630-7643AB	06 30 46.61	−76 43 08.9	0.483	356.8	14.82J	13.08J	11.00J	4	8.89J	8.28J	7.92J	6.9	2.0	11	5.5	0.9	12	12.5	M5.0V	2, 3	bc
SCR0631-8811	06 31 31.04	−88 11 36.6	0.516	349.9	15.65	14.05	12.04	3	10.04	9.46	9.07	12.8	5.1	11	10.4	1.6	12	25.5	M5.0V	3	
SCR0635-6722	06 35 48.81	−67 22 58.5	0.383	340.0	11.54	10.62	9.64	2	8.54	7.96	7.69	22.7	6.3	11	26.1	4.2	11	47.3	M0.5V	5	
SCR0640-0552	06 40 13.99	−05 52 23.3	0.592	170.5	10.22	9.22	8.03	3	6.84	6.21	5.96	8.5	2.3	11	9.3	1.5	12	26.2	M1.5V	4	d
SCR0642-6707	06 42 27.17	−67 07 19.8	0.811	120.4	16.01	14.43	12.42	3	10.62	10.15	9.81	24.1	12.0	11	17.6	3.9	12	67.8	M5.0V	3	
SCR0643-7003	06 43 29.79	−70 03 20.8	0.193	005.2	12.92	11.76	10.29	2	8.85	8.28	7.97	16.2	4.4	11	15.3	2.4	12	14.0	...	6	
SCR0644-4223AB	06 44 32.09	−42 23 45.2	0.197	163.8	14.44J	13.19J	11.55J	2	9.93J	9.27J	8.98J	18.8	5.2	11	17.5	2.9	12	16.3	...	6	e
SCR0702-6102	07 02 50.34	−61 02 47.6	0.786	041.4	16.62	14.75	12.49	3	10.36	9.85	9.52	15.9	7.6	11	10.8	2.0	12	40.2	M6.0V	2, 3	
SCR0713-0511	07 13 11.23	−05 11 48.6	0.304	183.6	11.13	10.08	8.86	3	7.65	7.08	6.82	13.1	4.7	10	13.5	2.1	12	19.4	M1.5V	6	
SCR0717-0500	07 17 17.09	−05 01 03.6	0.580	133.6	13.29	12.02	10.39	3	8.87	8.35	8.05	15.9	5.8	8	13.2	2.2	12	36.2	M4.0V	4	
SCR0723-8015	07 23 59.65	−80 15 17.8	0.828	330.4	17.41	15.61	13.41	2	11.30	10.82	10.44	19.3	5.6	11	17.1	3.1	12	67.2	M5.5V	2, 3	
SCR0736-3024	07 36 56.68	−30 24 16.4	0.424	145.7	13.64	12.41	10.83	2	9.36	8.79	8.50	20.2	9.0	11	17.3	2.7	12	34.7	M3.5V	4	
SCR0740-4257	07 40 11.80	−42 57 40.3	0.714	318.1	13.81	12.36	10.50	3	8.68	8.09	7.77	10.0	2.9	11	7.2	1.1	12	24.5	M4.5V	4	f
SCR0754-3809	07 54 54.84	−38 09 37.8	0.401	351.4	15.46	13.91	11.98	3	10.01	9.42	9.08	12.0	3.5	11	11.3	1.7	12	21.4	M4.5V	4	
SCR0805-5912	08 05 46.17	−59 12 50.4	0.637	155.0	14.69	13.38	11.68	3	10.07	9.52	9.22	20.4	6.0	11	19.4	3.1	12	58.7	M4.0V	3	
SCR0838-5855	08 38 02.24	−58 55 58.7	0.320	188.9	17.15	15.08	12.78	2	10.31	9.71	9.27	8.5	2.5	11	8.0	1.3	12	12.1	M6.0V	5	
SCR0914-4134	09 14 17.42	−41 34 37.9	0.749	312.5	15.01	13.57	11.72	3	9.98	9.42	9.12	18.2	8.0	11	14.6	2.4	12	51.9	M4.5V	4	
SCR1107-3420B	11 07 50.25	−34 21 00.6	0.287	167.0	15.04	13.68	11.96	3	10.26	9.70	9.41	19.2	5.5	11	19.1	3.0	12	26.0	M4.0V	6	gh
SCR1110-3608	11 10 29.01	−36 08 24.5	0.527	268.6	15.76	14.38	12.64	2	10.93	10.34	10.00	22.3	7.1	12	23.8	3.7	12	59.5	...	4	i
SCR1125-3834	11 25 37.27	−38 34 43.0	0.586	252.1	14.57	13.29	11.67	2	10.09	9.51	9.19	18.1	5.4	11	20.5	3.2	12	56.8	...	4	j
SCR1138-7721	11 38 16.76	−77 21 48.5	2.141	286.7	14.78	13.20	11.24	4	9.40	8.89	8.52	8.8	2.7	11	9.4	1.7	12	95.8	M5.0V	1, 2, 3	
SCR1147-5504	11 47 52.49	−55 04 11.9	0.192	011.3	13.72	12.54	11.06	2	9.67	9.08	8.81	24.2	8.1	11	23.1	3.6	12	21.0	...	5	
SCR1157-0149	11 57 45.55	−01 49 02.6	0.451	116.4	15.99	14.54	12.68	2	10.91	10.35	10.02	22.2	6.5	11	21.3	3.4	12	45.6	M4.5V	4	
SCR1204-4037	12 04 15.52	−40 37 52.6	0.695	150.0	13.47	12.34	10.92	2	9.57	9.02	8.75	21.2	5.7	11	25.2	3.9	12	83.0	...	4	k
SCR1206-3500	12 06 58.52	−35 00 52.0	0.422	229.3	14.67	13.35	11.66	2	10.01	9.40	9.13	21.0	5.9	11	17.7	2.7	12	35.4	...	4	
SCR1214-4603	12 14 39.98	−46 03 14.3	0.750	250.8	15.66	14.14	12.23	3	10.32	9.75	9.44	18.0	6.9	11	14.2	2.2	12	50.5	...	4	
SCR1217-7810	12 17 26.93	−78 10 45.9	0.212	056.6	16.43	14.92	13.05	2	11.20	10.64	10.36	24.5	8.6	11	23.3	3.8	12	23.4	...	5	

Table 3
(Continued)

Name	R.A.	Decl.	μ ($''$yr^{-1})	P.A. (°)	V_J	R_{KC}	I_{KC}	No. of Nights	J	H	K_s	d_{plt} (pc)	σ_{plt} (pc)	No. of Relations	d_{ccd} (pc)	σ_{ccd} (pc)	No. of Relations	V_{tan} (km s^{-1})	SpType	Reference	Notes
(1)	(2)	(3)	(4)	(5)	(6)	(7)	(8)	(9)	(10)	(11)	(12)	(13)	(14)	(15)	(16)	(17)	(18)	(19)	(20)	(21)	(22)
SCR1220-8302	12 20 03.71	−83 02 29.2	0.243	244.2	15.71	14.35	12.62	2	10.97	10.39	10.07	25.0	8.8	11	26.3	4.1	12	30.3	...	5	
SCR1224-5339	12 24 24.44	−53 39 08.8	0.189	251.9	15.31	13.95	12.19	2	10.51	9.93	9.65	18.2	5.5	11	21.0	3.3	12	18.8	...	5	
SCR1230-3411	12 30 01.75	−34 11 24.1	0.527	234.9	14.16	12.81	11.07	3	9.34	8.77	8.44	12.6	3.7	11	11.7	1.8	12	29.3	...	4	l
SCR1240-8116	12 40 56.02	−81 16 31.0	0.492	279.8	14.11	12.89	11.28	3	9.73	9.16	8.89	19.2	6.1	11	19.2	2.9	12	44.7	M4.0V	3	
SCR1245-5506	12 45 52.53	−55 06 50.2	0.412	107.0	13.66	12.32	10.61	3	8.99	8.43	8.12	11.5	3.4	11	11.3	1.8	12	22.1	M4.0V	3	
SCR1247-0525	12 47 14.73	−05 25 13.2	0.722	319.8	14.77	13.44	11.72	2	10.13	9.62	9.29	24.2	9.6	11	20.3	3.5	12	69.4	M4.0V	4	
SCR1347-7610	13 47 56.80	−76 10 20.0	0.194	089.7	11.49	10.57	9.66	3	8.62	8.01	7.77	22.6	6.2	11	29.2	4.7	9	26.8	...	5	
SCR1420-7516	14 20 36.84	−75 16 05.9	0.195	243.7	13.78	12.55	10.95	2	9.44	8.91	8.63	21.4	6.7	11	17.9	2.9	12	16.6	...	5	
SCR1441-7338	14 41 14.42	−73 38 41.4	0.207	029.0	16.96	15.31	13.25	2	11.20	10.61	10.27	19.0	5.5	11	17.2	2.7	12	16.8	...	5	
SCR1444-3426	14 44 06.56	−34 26 47.2	0.451	187.7	14.17	12.89	11.26	2	9.74	9.18	8.88	24.0	7.5	11	18.8	3.0	12	40.1	...	4	m
SCR1448-5735	14 48 39.82	−57 35 17.7	0.202	188.8	11.15	10.47	9.92	2	9.15	8.56	8.43	18.3	17.5	6	62.4	9.7	6	59.7	...	5	
SCR1450-3742	14 50 02.85	−37 42 09.8	0.449	212.2	14.01	12.84	11.32	2	9.95	9.37	9.07	21.2	6.0	11	25.9	4.2	12	55.1	...	4	n
SCR1456-7239	14 56 02.29	−72 39 41.4	0.207	225.0	15.36	13.99	12.28	2	10.62	10.06	9.74	24.9	7.0	11	22.8	3.6	12	22.4	...	5	
SCR1511-3403	15 11 38.63	−34 03 16.6	0.561	202.9	14.45	13.22	11.60	2	10.05	9.42	9.13	16.1	7.4	11	20.5	3.2	12	54.4	...	4	o
SCR1532-3622	15 32 13.90	−36 22 30.9	0.438	235.4	14.03	12.89	11.45	2	10.10	9.54	9.28	23.0	10.3	11	31.5	5.0	12	65.4	...	4	p
SCR1601-3421	16 01 55.68	−34 21 56.8	0.683	118.3	16.18	14.71	12.86	2	10.96	10.33	9.98	20.2	11.9	11	18.7	3.0	12	60.4	...	4	q
SCR1630-3633AB	16 30 27.23	−36 33 56.1	0.413	249.2	14.95J	13.47J	11.59J	2	10.04J	9.50J	9.03J	14.8	5.9	11	15.4	3.8	12	30.1	...	4	r
SCR1637-4703	16 37 56.62	−47 03 44.4	0.503	215.4	14.77	13.57	12.04	3	10.60	10.04	9.70	20.8	13.7	9	32.0	5.1	12	76.2	...	4	
SCR1726-8433	17 26 22.90	−84 33 08.2	0.518	134.8	14.25	13.00	11.41	2	9.87	9.33	9.02	20.1	5.5	11	20.6	3.2	12	50.6	M4.0V	3	
SCR1738-5942	17 38 41.02	−59 42 24.4	0.280	148.2	14.95	13.65	11.96	2	10.38	9.83	9.58	20.8	6.0	11	24.0	4.0	12	31.9	...	5	
SCR1746-8211	17 46 21.54	−82 11 56.6	0.228	184.9	12.44	11.33	9.91	2	8.55	7.99	7.71	14.6	4.0	11	15.5	2.4	12	16.7	...	5	s
SCR1820-6225	18 20 49.35	−62 25 52.7	0.190	164.8	12.04	11.12	10.17	2	9.14	8.49	8.30	22.5	9.5	8	36.6	5.8	10	33.0	...	5	
SCR1826-6542	18 26 46.83	−65 42 39.9	0.311	178.9	17.35	15.28	12.96	3	10.57	9.96	9.55	9.2	2.5	11	9.3	1.5	12	13.7	...	5	
SCR1841-4347	18 41 09.81	−43 47 32.8	0.790	264.2	16.46	14.72	12.59	3	10.48	9.94	9.60	14.6	4.3	11	11.9	2.0	12	44.5	...	4	
SCR1845-6357AB	18 45 05.26	−63 57 47.8	2.558	074.7	17.40J	14.99J	12.46J	5	9.54J	8.97J	8.51J	3.5	1.2	6	4.6	0.8	10	56.3	M8.5V	1, 2, 3	tu
SCR1847-1922	18 47 16.69	−19 22 20.8	0.626	230.7	14.35	13.11	11.48	2	9.91	9.38	9.09	23.0	6.6	11	20.6	3.2	12	61.1	...	4	
SCR1853-7537	18 53 26.61	−75 37 39.8	0.304	168.7	11.18	10.29	9.41	2	8.34	7.73	7.50	20.1	6.1	11	25.9	4.4	10	37.3	...	5	v
SCR1855-6914	18 55 47.89	−69 14 15.1	0.832	145.3	16.61	14.79	12.66	3	10.47	9.88	9.51	12.5	4.5	11	10.7	1.7	12	42.1	M5.5V	3	
SCR1856-4704AB	18 56 38.40	−47 04 58.3	0.252	131.3	14.85J	13.55J	11.87J	2	10.29J	9.75J	9.45J	21.4	6.2	11	22.6	3.6	12	27.0	...	5	w
SCR1926-8216AB	19 26 48.64	−82 16 47.6	0.195	172.5	11.29J	10.55J	9.89J	3	9.04J	8.43J	8.31J	17.3	4.7	3	53.4	8.5	6	49.3	...	5	x
SCR1931-0306	19 31 04.61	−03 06 18.0	0.578	031.0	16.81	15.11	13.11	3	11.15	10.56	10.23	18.0	4.8	6	18.0	3.0	12	49.2	M5.0V	4	
SCR1932-0652	19 32 46.33	−06 52 18.1	0.318	193.3	13.97	12.83	11.34	2	9.94	9.36	9.10	23.7	9.1	11	26.7	4.1	12	40.2	...	6	
SCR1932-5005	19 32 48.64	−50 05 38.9	0.257	157.5	15.47	14.14	12.42	2	10.75	10.11	9.85	24.4	7.8	11	23.5	3.7	12	28.6	...	5	
SCR1959-3631	19 59 21.03	−36 31 03.7	0.436	158.1	11.07	10.19	9.31	2	8.24	7.62	7.41	19.8	5.4	8	25.0	4.3	10	51.6	...	4	y
SCR1959-6236	19 59 33.55	−62 36 13.4	0.189	288.7	16.27	14.82	12.96	2	11.07	10.49	10.23	24.4	7.2	11	21.9	3.4	12	19.6	...	5	
SCR2009-0113	20 09 18.24	−01 13 38.2	0.381	186.2	14.47	12.98	11.16	3	9.40	8.83	8.51	14.0	4.4	11	10.8	1.8	12	19.5	...	6	
SCR2016-7531	20 16 11.25	−75 31 04.5	0.253	081.3	15.84	14.28	12.35	3	10.47	9.86	9.51	16.2	4.8	11	14.3	2.3	12	17.1	...	5	z
SCR2018-3635	20 18 06.52	−36 35 27.7	0.237	125.0	14.63	13.38	11.75	2	10.21	9.67	9.44	20.7	6.9	11	24.9	4.1	12	28.0	...	6	
SCR2025-2259	20 25 18.93	−22 59 06.0	0.191	219.5	14.22	13.03	11.48	2	10.00	9.48	9.16	23.5	7.0	11	24.6	3.8	12	22.2	...	6	
SCR2033-4903	20 33 01.87	−49 03 10.6	0.261	150.4	15.34	13.85	11.98	2	10.11	9.52	9.19	16.5	6.4	11	13.2	2.1	12	16.4	...	6	
SCR2040-5501	20 40 12.38	−55 01 25.6	0.514	125.4	15.22	13.91	12.22	2	10.56	10.02	9.69	22.9	6.9	11	23.3	3.6	12	56.8	M4.0V	3	
SCR2042-5737AB	20 42 46.44	−57 37 15.3	0.264	142.6	14.12J	12.89J	11.33J	3	9.97J	9.53J	9.03J	22.7	8.5	11	25.3	6.0	12	31.6	...	5	A
SCR2104-5248	21 04 53.85	−52 48 34.3	0.326	182.7	13.66	12.52	11.08	2	9.72	9.10	8.83	22.1	6.4	11	24.5	3.8	12	37.9	...	6	
SCR2105-5503	21 05 13.78	−55 03 56.3	0.334	171.0	13.97	12.69	11.05	2	9.59	8.92	8.64	17.1	4.8	11	16.7	2.8	12	26.4	...	6	
SCR2122-4314	21 22 16.92	−43 14 05.0	0.262	184.7	13.39	12.17	10.61	3	9.13	8.53	8.21	17.0	4.7	11	14.9	2.3	12	18.5	...	6	
SCR2130-7710	21 30 07.00	−77 10 37.5	0.589	118.0	17.01	15.33	13.31	2	11.29	10.67	10.37	20.6	7.3	11	18.4	2.9	12	51.3	M4.5V	3	B

Table 3
(Continued)

Name	R.A.	Decl.	μ ($''$yr^{-1})	P.A. ($^\circ$)	V_J	R_{KC}	I_{KC}	No. of Nights	J	H	K_s	d_{plt} (pc)	σ_{plt} (pc)	No. of Relations	d_{ccd} (pc)	σ_{ccd} (pc)	No. of Relations	V_{tan} (km s^{-1})	SpType	Reference	Notes
(1)	(2)	(3)	(4)	(5)	(6)	(7)	(8)	(9)	(10)	(11)	(12)	(13)	(14)	(15)	(16)	(17)	(18)	(19)	(20)	(21)	(22)
SCR2135-5325	21 35 39.63	−53 25 31.5	0.191	332.4	15.88	14.39	12.54	2	10.80	10.25	9.92	20.8	6.7	11	20.7	3.6	12	18.8	...	6	
SCR2142-7405	21 42 58.54	−74 05 55.5	0.210	162.1	13.06	12.02	10.74	2	9.46	8.78	8.58	21.9	6.3	11	26.7	4.5	12	26.5	...	6	
SCR2230-5244	22 30 27.95	−52 44 29.1	0.369	125.7	17.37	15.91	13.88	2	11.85	11.24	10.91	24.7	7.1	6	24.8	4.2	12	43.4	...	5	
SCR2241-6119A	22 41 44.36	−61 19 31.2	0.184	124.0	14.41	13.21	11.66	2	10.21	9.61	9.35	23.2	7.3	11	26.6	4.1	12	23.2	...	5	
SCR2241-6119B	22 41 43.67	−61 19 39.4	0.287	108.0	19.15	17.23	14.96	2	12.64	12.05	11.68	27.8	16.5	11	26.2	4.1	12	35.6	...	5	C
SCR2252-2220	22 52 25.82	−22 20 06.8	0.299	187.6	13.71	12.56	11.10	2	9.70	9.11	8.86	21.3	5.7	11	24.1	3.7	12	34.2	...	6	
SCR2301-5530	23 01 32.51	−55 30 17.6	0.338	052.8	12.65	11.57	10.25	2	8.98	8.36	8.13	15.1	4.5	11	21.4	3.3	12	34.3	...	6	
SCR2307-8452	23 07 19.67	−84 52 03.9	0.613	097.2	15.13	13.76	12.00	2	10.36	9.81	9.47	20.6	5.9	11	19.9	3.2	12	57.8	M4.0V	3	
SCR2325-6740	23 25 25.13	−67 40 07.9	0.284	123.2	14.38	13.11	11.48	2	9.91	9.33	9.05	20.0	5.7	11	19.5	3.0	12	26.2	...	6	D
SCR2335-6433A	23 35 18.43	−64 33 42.4	0.196	103.1	11.20	10.42	9.64	2	8.64	8.02	7.86	24.5	6.9	8	35.9	6.4	9	33.3	...	5	
SCR2335-6433B	23 35 19.95	−64 33 22.3	0.196	099.1	15.65	14.49	13.00	2	11.60	11.02	10.76	57.6	15.4	11	56.7	8.8	12	52.7	...	5	E

Notes. Coordinates are epoch and equinox 2000.0 using SuperCOSMOS positions transformed to epoch 2000.0 using the proper motions and position angles listed here; if AB, photometry or spectral type is for the system, i.e., joint.

[a] BD −08 409.
[b] AB separation 1″.
[c] SIPS J0630-7643.
[d] BD −05 1737.
[e] Angular separation of 1.″6 at a position angle of 266.°4.
[f] LSR J07401-4257.
[g] SCR1107-3420A is a white dwarf.
[h] Angular separation of 30.″6 at a position angle of 107.°1.
[i] LSR J11104-3608.
[j] LSR J11256-3834.
[k] LSR J12042-4037.
[l] LSR J12300-3411.
[m] LSR J14441-3426.
[n] LSR J14500-3742.
[o] LSR J15116-3403.
[p] LSR J15322-3622.
[q] LSR J16019-3421.
[r] Angular separation of 2″ at a position angle of 247.°2.
[s] Possible companion to HD158866 at 76.″5 at a position angle of 290.°8.
[t] DENIS-P J184504.9-635747.
[u] Angular separation of 1.″2 at a position angle of 170.°2.
[v] USNO-B1.0 0143-00184491.
[w] Angular separation of 1.″1 at a position angle of 139.°9.
[x] Angular separation of 1.″4 at a position angle of 238.°8.
[y] CD −36 13808.
[z] SIPS J2016-7531.
[A] Angular separation of 2.″2 at a position angle of 338.°4.
[B] SIPS J2130-7710.
[C] Angular separation of 9.″6 at a position angle of 211.°2.
[D] LEHPM 5810.
[E] Angular separation of 22.″4 at a position angle of 25.°9.

References. (1) Hambly et al. 2004; (2) Henry et al. 2004; (3) Subasavage et al. 2005a; (4) Subasavage et al. 2005b; (5) Finch et al. 2007; (6) this paper.

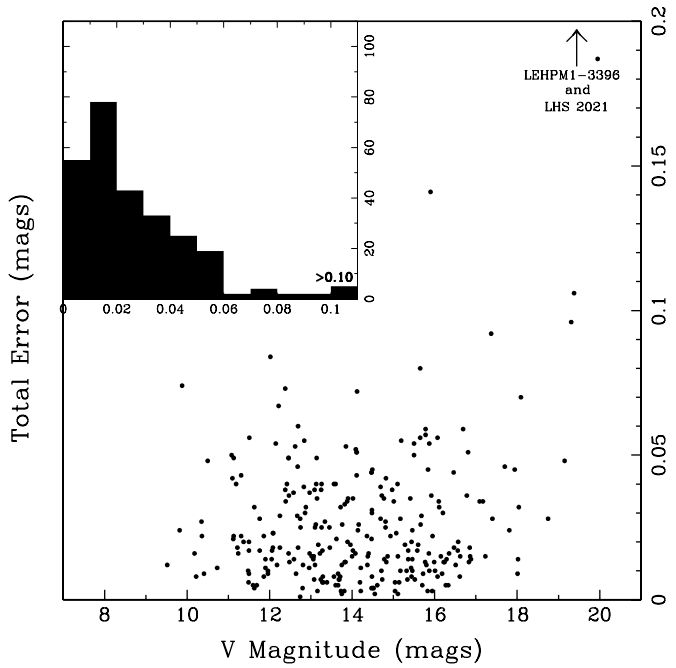

Figure 2. Total CCD photometric errors vs. *V* magnitude for the CTIO 0.9 m telescope data. Inset at the upper left is a histogram of the number of objects in each error bin. The total number of objects plotted is 268 (including some of the SCR objects presented in this paper), and each error bin is 0.01 mag. The arrow at the upper right of the figure indicates that LEHPM1-3396 ($V = 19.38$) and LHS 2021 ($V = 19.21$) are both off the plot.

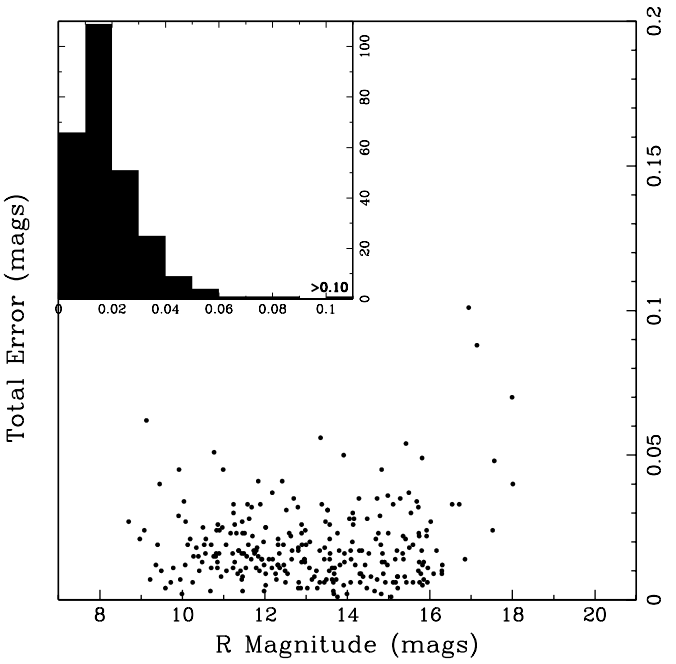

Figure 3. Same as Figure 2, but for CCD photometry in the *R* band.

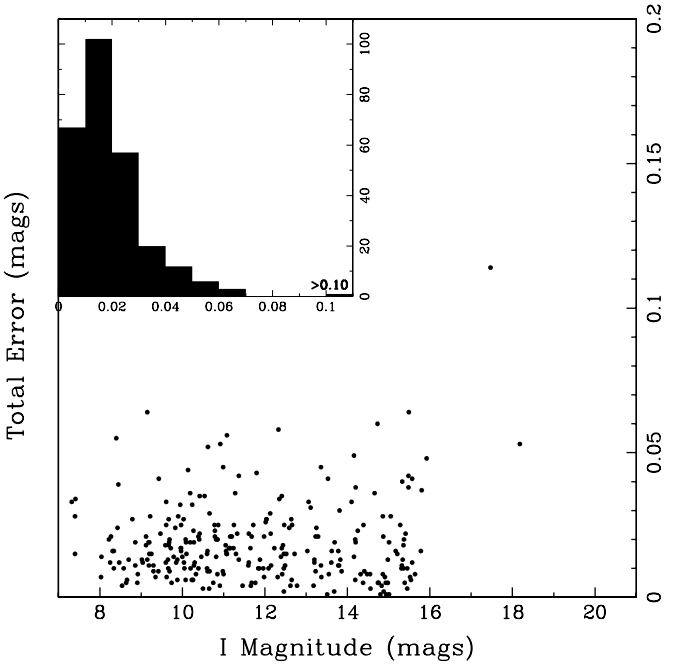

Figure 4. Same as Figure 2, but for CCD photometry in the *I* band.

0.05 mag or less for objects brighter than 16th mag at *V*, brighter than 18th mag at *R*, and brighter than 17th mag at *I*. Standard star fits on most nights have errors of 0.01–0.02 mag. Typical variations in photometric measurements from night to night are 0.02–0.03 mag. As can be seen in Figures 2–4, the convolution of all three errors typically results in total errors of 0.03 mag or less for 66% of objects at *V* and 84% of objects at both *R* and *I*, as evident from the inset histograms. Note that the lack of a general increase in errors for fainter stars is caused by observers increasing integration times to provide adequate signal to noise on even the faintest targets. Nonetheless, these red dwarfs are faintest at *V*, so the resulting errors are somewhat larger than at *R* and *I*. At *V*, 94% of the objects presented have total errors of 0.06 mag or less; for *R* and *I*, this statistic is 99%. The SCR systems reported here follow the general trend reported above: the fraction of objects with errors less than 0.03 mag is 73%, 94%, and 92%, respectively, at *VRI*. At *V*, 94% of the objects have total errors less than 0.06 mag, while this is true of 100% of the objects at *R* and *I*.

4.2. JHK Photometry from 2MASS

Infrared photometry in the JHK_s system has been extracted from 2MASS and is rounded to the nearest hundredth magnitude. The same 2MASS photometry has been used for both the plate distance estimates and new CCD distance estimates presented here. The JHK_s magnitude errors listed are the x_sigcom errors (where x is j, h, or k) and include target, global, and systematic influences. These errors are generally less than 0.04 mag. Exceptions at *H* are SCR0214-0733 (0.05 mag), SCR0211-6108, SCR1230-3411, and SCR0717-0500 (all 0.06 mag).

4.3. CCD Distance Estimates

The CCD distance estimates,[14] as described in Henry et al. (2004), are found using a method similar to that used for the photographic plate distance estimates. The difference is that we use the accurate *VRI* magnitudes obtained at CTIO instead of *BRI* plate magnitudes from SuperCOSMOS. The maximum number of relations possible from the combination of *VRIJHK* magnitudes is 15 (the same number of combinations as for the plate relations), but only 12 yield useful results. The color spread

[14] The term "CCD distance estimate" is used for the remainder of the paper to indicate a CCD photometric distance estimate.

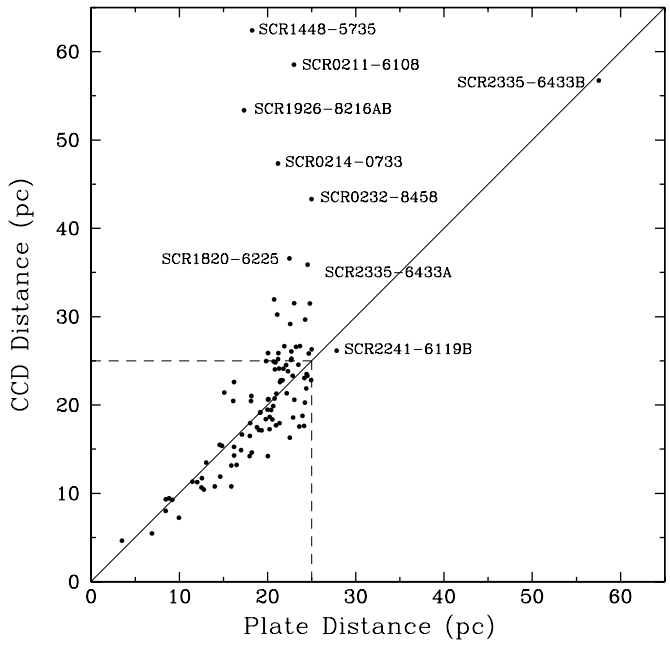

Figure 5. CCD distance vs. plate distance without error bars. A solid diagonal line represents CCD distance estimates exactly matching photographic plate distance estimates. The dashed line is a 25.0 pc boundary, indicating the ultimate distance horizon of interest for this sample. Outliers have been labeled.

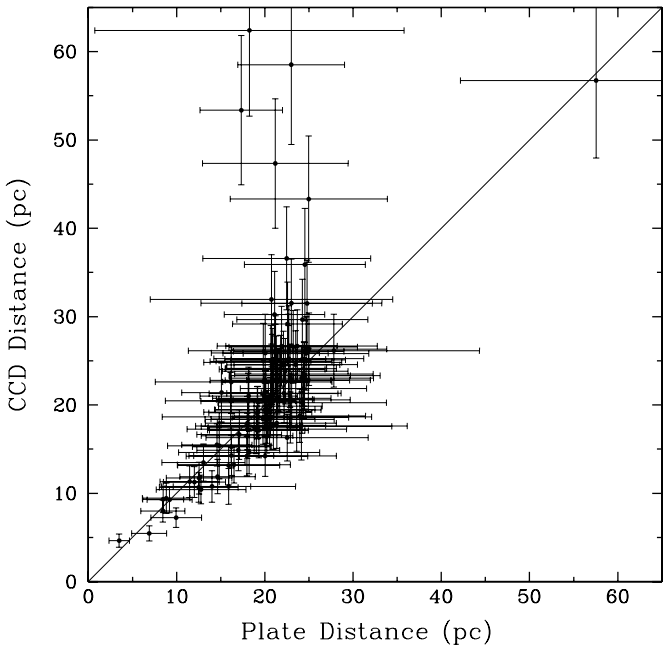

Figure 6. CCD distance vs. plate distance with error bars. The total errors for photographic plate distance estimates include the standard deviation of the (up to) 11 individual distance estimates plus 26% systematic errors incorporated primarily because of cosmic scatter. Similarly, the total errors for CCD distance estimates include the standard deviation of the (up to) 12 individual distance estimates plus 15% systematic errors incorporated primarily because of cosmic scatter.

is not large enough in three of the relations (M_K versus $J-H$, $J-K$, and $H-K$) to give reliable results and so are omitted.

Of the 100 systems with photographic plate distance estimates that place them closer than 25.0 pc, we find 77 to have CCD distance estimates within the 25.0 pc horizon. Thus, we retain 77% of the SuperCOSMOS discoveries as likely nearby stars. All systems with CCD distance estimates within 15.0 pc and additional compelling systems are targeted for trigonometric parallax measurements as part of our Cerro Tololo Inter-American Observatory Parallax Investigation (CTIOPI) (Jao et al. 2005; Henry et al. 2006; Subasavage et al. 2009; Riedel et al. 2010). At present, 31 of the systems discussed here are on the CTIOPI program.

Figure 5 shows a comparison of the two photometric distance estimates with error bars omitted for clarity. Primary stars and a few secondaries for which separate photometry is available are plotted. The single point in the upper right of the plot and one point with a plate distance estimate of 25–30 pc are secondary components (SCR2241-6119B and SCR2335-6433B). Twenty-three systems are estimated to be beyond 25 pc using CCD distance estimates. The two most likely causes of the distance offsets are poor plate photometry compared to CCD photometry and close multiples that are unresolved on the plates but resolved in CCD images. Errors in the plate photometry certainly cause most of the discrepancies. A distance of up to ∼35 pc is possible if the object is an unresolved binary in which the two components are identical and contribute an equal amount of light to the measured magnitude. All SCR targets have been inspected for duplicity in the CCD images. Seven were found to be binaries with separations between 1″ (typical resolution of our CCD images) and 5″. The typical resolution of the plate images for binaries with magnitude differences of $\lesssim 2$ is 4″. Details on multiple systems can be found in Section 5.1.

Eight objects are found to have CCD distance estimates of 35–65 pc. One object (SCR2335-6433B in the upper right of Figures 5 and 6) is a common proper motion companion that was discovered by eye when blinking plates. The remaining seven objects had 3–8 plate relations contributing to their distance estimates rather than the full suite of 11, indicative of inaccurate estimates. The corresponding CCD distances for these objects often rely on 6–10 relations rather than the full suite of 12, typically because they are bluer than some of the plate and CCD distance relations. Three of the eight objects have already been verified to be K dwarfs via spectroscopy.

4.4. Photometric Distance Estimate Errors

When using both the plate and CCD distance estimating suites, there is inherent spread around the fit line for each relation that is a result of two causes: (1) the deviations due to errors in parallax and photometry for the stars used to derive the fits, and (2) cosmic scatter due to differences in stellar ages, compositions, and perhaps magnetic properties. Cosmic scatter dominates the offsets between distance estimates and true distances. Unresolved, unknown multiples may also contribute, although great care was taken to remove such systems before the fits were made, so this is not a significant issue. In order to estimate the reliability of the suites of relations in both the plate and CCD methods, we have run single, main-sequence, red dwarfs with known trigonometric distances back through the relations to derive representative errors. The median offsets between the trigonometric and photometric distance estimates are 26% for the plate suite and 15% for the CCD suite.

For all errors on distance estimates listed in Table 3, these percentage errors are combined in quadrature with each star's individual error, which comes from the up to 11 or 12 distances derived from the plate and CCD suites, respectively. Figure 6 is the same as Figure 5, but with the total errors shown for both estimates. Note that in no case can the plate distance estimate

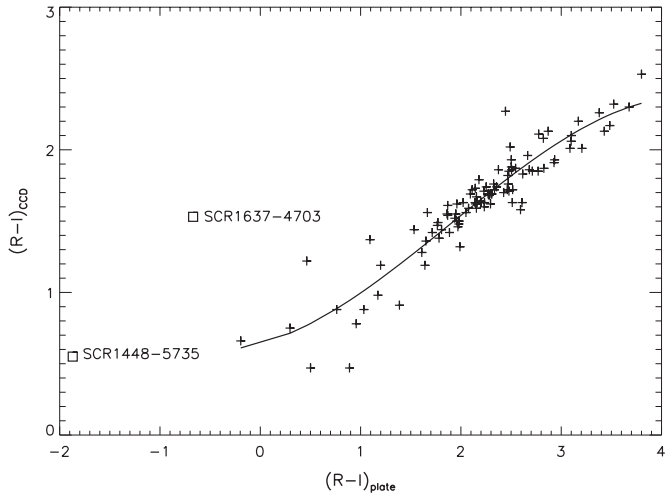

Figure 7. CCD ($R-I$) color vs. plate ($R-I$) color with a polynomial fit for 100 SCR objects. The two outliers, denoted by open squares and labeled, were not used in the fit due to blending on the R plates, nor were two objects for which no I plate magnitude was available (SCR1931-0306 and SCR2230-5244).

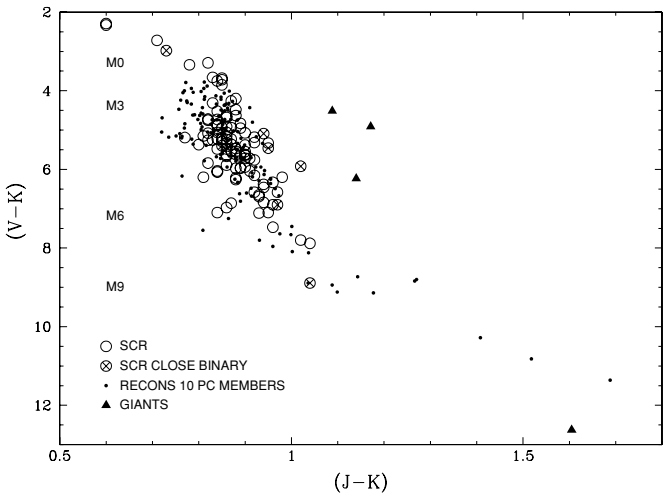

Figure 8. Color–color diagram of ($V-K$) vs. ($J-K$). Spectral type estimates are listed inside the y-axis. Open circles indicate 104 SCR objects presented in this paper; for the two resolved binary systems (SCR2241-6119AB and SCR2335-6433AB), photometry is available for both components. ×'s surrounded by open circles symbolize confirmed SCR binaries with combined photometry. Known RECONS 10 pc sample systems are shown as solid dots, and known giants are denoted by solid triangles.

have an error less than 26% nor less than 15% for the CCD distance estimate.

Figure 7 illustrates a comparison of the SuperCOSMOS plate ($R-I$) color and the CCD ($R-I$) color for 100 SCR stars reported here. The fit is a polynomial described by $(R-I)_{\rm ccd} = 0.640 + 0.192*(R-I)_{\rm plate} + 0.198*(R-I)^2_{\rm plate} - 0.035*(R-I)^3_{\rm plate}$. This polynomial permits users of SuperCOSMOS data to predict the $(R-I)_{\rm ccd}$ color that would be measured for red objects, i.e., those with $-0.2 = (R-I)_{\rm plate} = 3.8$.

Two outlying points represented by open squares are SCR1448-5735 and SCR1637-4703, both of which were omitted from the fit because they are blended with other sources in R images. Two other objects for which I plate magnitudes were not available (SCR1931-0306 and SCR2230-5244) were also excluded from the fit. The mean absolute deviation is 0.27 mag, indicating that the SuperCOSMOS ($R-I$) color is roughly nine times less accurate than the CCD ($R-I$) color, which typically has errors less than 0.03 mag.

5. CONFIRMATION AS RED DWARFS: SPECTROSCOPY AND THE COLOR–COLOR DIAGRAM

For 37 stars, we have spectra that were acquired on the CTIO 1.5 m between 2003 July and 2006 December. Observations were made using a 2.″0 slit or wider in the RC Spectrograph with grating 32 and order blocking filter OG570 to provide wavelength coverage from 6000 to 9500 Å and resolution of 8.6 Å on the Loral 1200 × 800 CCD. Reductions were performed using standard procedures via IRAF. Spectral types have been assigned on the RECONS system (Jao et al. 2008). Thirty-four of the stars are confirmed to be M dwarfs, while three are K dwarfs. The three K dwarfs have slipped into the sample because of erroneous plate magnitudes, as evidenced by having fewer than 11 relations for their plate distance estimates.

For all of the stars, we use a color–color diagram to verify that the sample objects are red dwarfs. Figure 8 is a color–color diagram that plots ($V-K$) versus ($J-K$). Labels denoting spectral types are shown inside the left axis. SCR stars are open circles, with the combined photometry of seven SCR close binaries marked by crosses inside the circles. The dots are RECONS 10 pc sample members (Henry et al. 2006), and a few known giants are plotted as solid triangles for reference. As is evident from this diagram, none of the SCR stars presented in this paper fall in the region where known giants are found, so we are relatively confident that none of these objects are giants. We anticipate that these objects are not subdwarfs because their tangential velocities are $\leqslant$100 km s^{-1}. The point that is slightly elevated (1.02, 5.90) toward the three giants is the binary system SCR1630-3633AB.

5.1. Multiples

Eleven of the systems presented in this paper are binary, with seven systems having separations less than 3″. Six of these close binaries are newly discovered via the SCR effort—SCR0630-7643AB, SCR0644-4223AB, SCR1630-3633AB, SCR1856-4704AB, SCR1926-8216AB, and SCR2042-5737AB—while SCR1845-6357A was discovered via the SCR effort and the companion first detected by Biller et al. (2006). Table 4 lists the binary data, including the separations of the components, position angles of the secondaries relative to the primaries, distance estimates of the system for close systems (indicated by brackets) and of the components where separate photometry was possible, and the distance errors.

All systems were re-blinked using the SuperCOSMOS photographic plates to ensure that no widely separated companions out to 5′ had been previously overlooked. No new discoveries were made. A search was then made for closer companions by examining all I frames taken at CTIO in IRAF, using the surface, contour, and radial plot features available. Separations were determined using the SExtractor (Bertin & Arnouts 1996) feature in IRAF, with some parameters (*detect_minarea, deblend_nthresh, deblend_mincont*) modified in order for the program to recognize both components of the close system. These results are listed in Table 4.

Two binary systems, SCR0630-7643AB and SCR1630-3633AB, have been confirmed to be physically related via *HST*-FGS (*Hubble Space Telescope* Fine Guidance Sensors) observations. The ΔV values between the two components in each

Table 4
Binary Data for SCR Sample

Name	Separation (″)	P.A. (deg)	d_{ccd} (pc)	σ_{ccd} (pc)	Notes
SCR0630-7643A			8.8	0.9	a
SCR0630-7643B	1.0	33.8	[5.5]	0.9	
SCR0644-4223A			[17.5]	2.9	
SCR0644-4223B	1.6	266.4	[17.5]	2.9	
SCR1107-3420A			28.2	3.0	b
SCR1107-3420B	30.6	107.1	19.1	3.0	b
SCR1630-3633A			[15.4]	3.8	
SCR1630-3633B	2.0	247.2	[15.4]	3.8	
HD158866			30.6	0.9	c
SCR1746-8211	76.5	290.8	15.5	2.4	c
SCR1845-6357A			3.9	0.8	a
SCR1845-6357B	1.2	170.2	[4.6]	0.8	d
SCR1856-4704A			[22.6]	3.6	
SCR1856-4704B	1.1	138.9	[22.6]	3.6	
SCR1926-8216A			[53.4]	8.5	
SCR1926-8216B	1.4	238.8	[53.4]	8.5	
SCR2042-5737A			[25.3]	6.0	
SCR2042-5737B	2.2	338.4	[25.3]	6.0	
SCR2241-6119A			26.6	4.1	e
SCR2241-6119B	9.6	211.2	26.2	4.1	e
SCR2335-6433A			35.9	6.4	e
SCR2335-6433B	22.4	25.9	56.7	8.8	e

Notes. Brackets around the distance estimate indicate that the estimate is for the system.
[a] Trigonometric parallax in Henry et al. (2006).
[b] Separation and position angle for the system and distance estimate for the primary (derived from the SED) are from Subasavage et al. (2007).
[c] Separation and position angle for the system from Finch et al. (2007); trigonometric distance for the primary is from van Leeuwen (2007) (HIPPARCOS).
[d] Separation and position angle for the system from Biller et al. (2006).
[e] Separation and position angle for the system from Finch et al. (2007).

system were estimated by comparing *HST*-FGS scans to systems in which the ΔV is known (Henry et al. 1999).

5.2. Objects Worthy of Note

SCR0630-7643AB has a photometric distance estimate of 5.5 pc, but has a trigonometric distance of 8.8 pc in Henry et al. (2006). This is a new close binary with a separation of 1.″0 and a $\Delta V \sim 0.3$ mag that has been confirmed with both continuing optical speckle and *HST*-FGS observations.

SCR1107-3420B is 30.″6 from the primary at a position angle of 107.°1; the primary component is a white dwarf with an estimated distance of 28.2 pc (Subasavage et al. 2007). No companions have been found for the red dwarf secondary by *HST*-FGS and speckle observations.

SCR1630-3633AB is a new binary system, confirmed by *HST*-FGS with $\Delta V \sim 0.7$ mag. A more realistic distance estimate is ∼20 pc, taking into consideration the system's multiplicity.

SCR1746-8211 was thought to be a possible common proper motion companion to HD 158866, at a separation of 76.″5 at 290.°8 (Finch et al. 2007). However, the distance estimate, 15.5 pc, is not in agreement with the distance of the primary, 30.6 pc, as measured by HIPPARCOS (van Leeuwen 2007). The proper motion of the primary, $\mu = 0.''211$ yr^{-1} at 191°, is inconsistent with that of the secondary, $\mu = 0.''288$ yr^{-1} at 184.°9. Thus, the two objects do not appear to be in the same system.

SCR1845-6357AB has a CCD distance estimate of 4.6 pc and a trigonometric parallax that revises the distance to 3.9 pc (Henry et al. 2006). This is the 24th closest system to the Sun, composed of M8.5 and T dwarfs at a separation of 1.″2 (Biller et al. 2006).

SCR2241-6119AB is a binary system separated by 9.″6 at 211.°2. The two components appear to be co-moving in SuperCOSMOS images, but the proper motion values do not match: A has $\mu = 0.''184$ yr^{-1} at 124.°0, while B has $\mu = 0.''287$ yr^{-1} at 108.°0. However, the B component is very faint in the *B* image, faint in the *R* image, and not round in the *I* image, likely leading to a poor, and inconsistent, proper motion measurement.

SCR2335-6433AB has a separation of 22.″4 at 25.°9 (Finch et al. 2007), making photometry for each component possible. However, the distance estimates for the A and B components, 35.9 and 56.7 pc, respectively, do not agree. This is likely due to the fact that only nine of the 12 CCD relations were in agreement for the primary. As all 12 relations were utilized in the distance estimate of the secondary, the true distance of the system is probably closer to that of the secondary.

Table 5
Distance Statistics for SCR Sample of M Dwarf Systems

Distance	No. of Systems	No. of Binaries[a]
$d \leqslant 5.0$ pc	1	1
$5.0 < d \leqslant 10.0$ pc	6	1
$10.0 < d \leqslant 15.0$ pc	16	0
$15.0 < d \leqslant 20.0$ pc	23	2
$20.0 < d \leqslant 25.0$ pc	31	1
$d \geqslant 25.0$ pc	23	4
TOTAL	100	9

Note. [a] Omitting SCR1107-3420B and SCR1746-8211, both of which have primaries that are not M dwarfs.

6. DISCUSSION

The majority of the objects (71 of 104, or 68% of the sample) have $V > 14$ because these new discoveries are fainter than those targeted by Luyten in most of the southern sky. Only the faint companion object discovered by eye during the blinking process, SCR2241-6119B ($R = 17.23$), is fainter than CCD $R = 16$, a consequence of the plate $R = 16.5$ cutoff chosen in our searches to date. The color–color diagram in Figure 8 shows that most of the 104 SCR objects are M3−M6 type dwarfs, which corresponds to the "sweet spot" created by our search magnitudes through most of the 25 pc volume.

As can be seen in the polar plot of Figure 1, many of these SCR discoveries are south of −60°. Luyten's Palomar survey for proper motion stars extended to −45° for a quarter of the southern sky and to −33° for the entire southern sky (Luyten 1974), and his Bruce Survey covered the remainder of the southern sky. Giclas searched declinations north of −45° for stars of magnitudes 8–17 with proper motions ⩾0.20 and at even smaller μ for red objects (Giclas et al. 1978a). Still, we have found 11 systems between decl. = 0° and −30°, an area of the sky covered previously by both Luyten and Giclas. Four of these 11 are brighter than $V = 14$ and so were missed by those surveys.

In total, the 77 systems we determine to be within 25 pc, when compared to the 329 southern systems found in NStars, result in a 23% increase in the number of red dwarf systems nearer than 25.0 pc in the southern sky. In Table 5, we summarize the distance distribution for the 100 systems discussed in this paper,

as well as the number of binaries found within each distance bin. We anticipate that seven will prove to be within 10 pc and 70 will be between 10 and 25 pc, while the remaining 23 systems are likely beyond 25 pc. If all of the new red dwarf systems from our SCR search to date, plus the 89 systems found by Phan-Bao et al., Reylé et al., Finch et al., and Costa & Méndez are found to have trigonometric parallaxes placing them within 25 pc, the number of red dwarf systems in the southern sky within that horizon would increase by 50%. Forthcoming in this series is a paper presenting trigonometric parallaxes for roughly one-third of the SCR systems in this paper, three of which (SCR0630-7643AB, SCR1138-7721, SCR1845-6357AB) have had results published previously (Henry et al. 2006).

We have several continuing efforts to reveal the Sun's red dwarf neighbors. We have found another ∼100 systems with $0\farcs40\ \mathrm{yr}^{-1} > \mu \geqslant 0\farcs18\ \mathrm{yr}^{-1}$ between decl. $= 0^\circ$ and -47° during our continuing sweep of the southern sky. This search is a complement to our Finch et al. (2007) effort and will complete the SCR search of the southern sky for stars that would have been members of Luyten's New Luyten Two-Tenths (NLTT) Catalogue (Luyten 1979b). Already underway is a project to gather photometric data for ∼150 additional SCR systems that have photographic plate distance estimates placing them between 25 and 30 pc. Some of these systems will, in effect, replace the 23 systems with CCD distances beyond the 25 pc original limit of the plate distances. Already, of the 38 systems for which we have obtained initial *VRI* photometry, nine are anticipated to be nearer than the 25 pc horizon. Still remaining are additional searches that probe beyond the $R = 16.5$ cutoff of our first sweep of the southern sky.

The support of additional RECONS team members was vital for this research, in particular Adric Riedel. We also thank Brian Mason for insight on preliminary optical speckle survey results, as well as Ed Nelan for early results from *HST*-FGS. This work has been supported under National Science Foundation grants AST 05-07711 and AST 09-08402, as well as by NASA's Space Interferometry Mission, and Georgia State University. We also thank the members of the SMARTS Consortium, who enable the operations of the small telescopes at CTIO, as well as the observer support at CTIO, especially Edgardo Cosgrove, Arturo Gomez, Alberto Miranda, and Joselino Vasquez. This research makes use of data products from the Two Micron All Sky Survey, which is a joint project of the University of Massachusetts and the Infrared Processing and Analysis Center/California Institute of Technology, funded by the National Aeronautics and Space Administration and the National Science Foundation. This research also makes use of the SIMBAD database and the Aladin and Vizier interfaces, operated at CDS, Strasbourg, France. Thank you to the referees for their helpful comments, as well.

REFERENCES

Adelman-McCarthy, J. K., et al. 2009, VizieR Online Data Catalog, 2294, 0
Bertin, E., & Arnouts, S. 1996, A&AS, 117, 393
Bessel, M. S. 1990, A&AS, 83, 357
Biller, B. A., Kasper, M., Close, L. M., Brandner, W., & Kellner, S. 2006, ApJ, 641, L141
Costa, E., & Méndez, R. A. 2003, A&A, 402, 541
Deacon, N. R., & Hambly, N. C. 2007, A&A, 468, 163
Deacon, N. R., Hambly, N. C., & Cooke, J. A. 2005, A&A, 435, 363
Delfosse, X., et al. 2001, A&A, 366, L13
Eggen, O. J. 1987, AJ, 93, 379
Finch, C. T., Henry, T. J., Subasavage, J. P., Jao, W.-C., & Hambly, N. C. 2007, AJ, 133, 2898
Finch, C. T., Zacharias, N., & Henry, T. J. 2010, AJ, 140, 844
Giclas, H. L., Burnham, R., Jr., & Thomas, N. G. 1971, Lowell Proper Motion Survey Northern Hemisphere. The G Numbered Stars (Flagstaff, AZ: Lowell Observatory)
Giclas, H. L., Burnham, R., Jr., & Thomas, N. G. 1978a, Lowell Obs. Bull., 8, 51
Giclas, H. L., Burnham, R., Jr., & Thomas, N. G. 1978b, Lowell Obs. Bull., 8, 89
Gliese, W., & Jahreiß, H. 1991, in The Astronomical Data Center CD-ROM: Selected Astronomical Catalogs, Vol. 1, ed. L. E. Brotzmann & S. E. Gesser (Greenbelt, MD: NASA)
Graham, J. A. 1982, PASP, 94, 244
Hambly, N. C., Henry, T. J., Subasavage, J. P., Brown, M. A., & Jao, W.-C. 2004, AJ, 128, 437
Hambly, N. C., Irwin, M. J., & MacGillivray, H. T. 2001, MNRAS, 326, 1295
Henry, T. J., Backman, D. E., Blackwell, J., Okimura, T., & Jue, S. 2003, Astrophysics and Space Science Library, 289, 111
Henry, T. J., Jao, W.-C., Subasavage, J. P., Beaulieu, T. D., Ianna, P. A., Costa, E., & Méndez, R. A. 2006, AJ, 132, 2360
Henry, T. J., Subasavage, J. P., Brown, M. A., Beaulieu, T. D., Jao, W.-C., & Hambly, N. C. 2004, AJ, 128, 2460
Henry, T. J., Walkowicz, L. M., Barto, T. C., & Golimowski, D. A. 2002, AJ, 123, 2002
Henry, T. J., et al. 1999, ApJ, 512, 864
Jao, W.-C., Henry, T. J., Beaulieu, T. D., & Subasavage, J. P. 2008, AJ, 136, 840
Jao, W.-C., Henry, T. J., Subasavage, J. P., Brown, M. A., Ianna, P. A., Bartlett, J. L., Costa, E., & Méndez, R. A. 2005, AJ, 129, 1954
Jao, W.-C., et al. 2010, AJ, submitted
Landolt, A. U. 1992, AJ, 104, 372
Landolt, A. U. 2007, AJ, 133, 2502
Lépine, S. 2005a, AJ, 130, 1247
Lépine, S. 2005b, AJ, 130, 1680
Lépine, S. 2008, AJ, 135, 2177
Luyten, W. J. 1974, in IAU Symp. 61, New Problems in Astrometry, ed. W. Gliese, C. A. Murray, & R. H. Tucker (Dordrecht: Reidel), 169
Luyten, W. J. 1979a, in LHS Catalogue, ed. W. J. Luyten (2nd ed.; Minneapolis, MN: Univ. Minnesota), 100
Luyten, W. J. 1979b, in NLTT Catalogue. Volume_I. +90__to_+30_. Volume._II. +30__to_0_., ed. W. J. Luyten (Minneapolis, MN: Univ. Minnesota), 282 (Vol. I), 286 (Vol. II)
Phan-Bao, N., Forveille, T., Martín, E. L., & Delfosse, X. 2006, ApJ, 645, L153
Phan-Bao, N., et al. 2001, A&A, 380, 590
Phan-Bao, N., et al. 2003, A&A, 401, 959
Phan-Bao, N., et al. 2008, MNRAS, 383, 831
Reid, I. N., Cruz, K. L., Kirkpatrick, J. D., Allen, P. R., Mungall, F., Liebert, J., Lowrance, P., & Sweet, A. 2008, AJ, 136, 1290
Reylé, C., & Robin, A. C. 2004, A&A, 421, 643
Reylé, C., Robin, A. C., Scholz, R.-D., & Irwin, M. 2002, A&A, 390, 491
Riedel, A. R., et al. 2010, AJ, 140, 897
Skrutskie, M. F., et al. 2006, AJ, 131, 1163
Subasavage, J. P., Henry, T. J., Bergeron, P., Dufour, P., Hambly, N. C., & Beaulieu, T. D. 2007, AJ, 134, 252
Subasavage, J. P., Henry, T. J., Hambly, N. C., Brown, M. A., & Jao, W.-C. 2005a, AJ, 129, 413
Subasavage, J. P., Henry, T. J., Hambly, N. C., Brown, M. A., Jao, W.-C., & Finch, C. T. 2005b, AJ, 130, 1658
Subasavage, J. P., Jao, W.-C., Henry, T. J., Bergeron, P., Dufour, P., Ianna, P. A., Costa, E., & Méndez, R. A. 2009, AJ, 137, 4547
The Denis Consortium 2005, VizieR Online Data Catalog, 1, 2002
van Leeuwen, F. 2007, Hipparcos, the New Reduction of the Raw Data (Astrophysics and Space Science Library, Vol. 350; Cambridge: Cambridge Univ. Press)
Weis, E. W. 1996, AJ, 112, 2300